Eur J Nucl Med Mol Imaging (2011) 38:920–929
DOI 10.1007/s00259-010-1721-9

ORIGINAL ARTICLE

The effect of patient positioning aids on PET quantification in PET/MR imaging

Frederic Mantlik · Matthias Hofmann · Matthias K. Werner · Alexander Sauter · Jürgen Kupferschläger · Bernhard Schölkopf · Bernd J. Pichler · Thomas Beyer

Received: 25 August 2010 / Accepted: 16 December 2010 / Published online: 10 February 2011

Abstract
Objectives Clinical PET/MR requires the use of patient positioning aids to immobilize and support patients for the duration of the combined examination. Ancillary immobilization devices contribute to overall attenuation of the PET signal, but are not detected with conventional MR sequences and, hence, are ignored in standard MR-based attenuation correction (MR-AC). We report on the quantitative effect of not accounting for the attenuation of patient positioning aids in combined PET/MR imaging.
Methods We used phantom and patient data acquired with positioning aids on a PET/CT scanner (Biograph 16, HI-REZ) to mimic PET/MR imaging conditions. Reference CT-based attenuation maps were generated from measured (original) CT transmission images (origCT-AC). We also created MR-like attenuation maps by following the same conversion procedure of the attenuation values except for the prior delineation and subtraction of the positioning aids from the CT images (modCT-AC). First, a uniform ^{68}Ge cylinder was positioned centrally in the PET/CT scanner and fixed with a vacuum mattress (10 cm thick) and, in a repeat examination, with MR positioning foam pads. Second, 16 patient datasets were selected for subsequent processing. All patients were regionally immobilized with positioning aids: a vacuum mattress for head/neck imaging (nine patients) and a foam mattress for imaging of the lower extremities (seven patients). PET images were reconstructed following CT-based attenuation and scatter correction using the original and modified (MR-like) CT images: $PET_{origCT\text{-}AC}$ and $PET_{modCT\text{-}AC}$, respectively. PET images following origCT-AC and modCT-AC were compared visually and in terms of mean differences of voxels with a standardized uptake value of at least 1.0. In addition, we report maximum activity concentration in lesions for selected patients.
Results In the phantom study employing the vacuum mattress the average voxel activity in $PET_{modCT\text{-}AC}$ was underestimated by 6.4% compared to $PET_{origCT\text{-}AC}$, with 3.4% of the PET voxels being underestimated by 10% or more. When the MR foam pads were not accounted for during AC, $PET_{modCT\text{-}AC}$ was underestimated by 1.1% on average, with none of the PET voxels being underestimated by 10% or more. Evaluation of the head/neck patient data showed a decrease of 8.4% ([^{68}Ga]DOTATOC) and 7.4% ([^{18}F]FDG) when patient positioning aids were not accounted for during AC, while the corresponding decrease was insignificant for the lower extremities.
Conclusion Depending on the size and density of the positioning aids used, a regionally variable underestimation

F. Mantlik (✉) · M. Hofmann · B. J. Pichler
Laboratory for Preclinical Imaging and Imaging Technology of the Werner Siemens-Foundation, Department of Radiology, University of Tübingen,
Roentgenweg 13,
72076 Tübingen, Germany
e-mail: frederic.mantlik@med.uni-tuebingen.de

F. Mantlik · M. Hofmann · B. Schölkopf
Max Planck Institute for Biological Cybernetics, Tübingen, Germany

M. K. Werner · A. Sauter
Department of Diagnostic and Interventional Radiology, University Hospital, Tübingen, Germany

J. Kupferschläger
Department of Nuclear Medicine, University Hospital, Tübingen, Germany

T. Beyer
Imaging Science Institute, University Hospital, Tübingen, Germany

of PET activity following AC is observed when positioning aids are not accounted for. This underestimation may become relevant in combined PET/MR imaging of patients with neuropsychiatric indications, but appears to be of no clinical relevance in imaging the extremities.

Keywords PET/MR · Attenuation · Positioning aids

Introduction

Recently, combined PET/MR systems have been proposed as a new approach to dual modality imaging of patients [1]. Today, prototype systems exist for simultaneous imaging of the brain [2] and for sequential acquisition of extended imaging ranges, such as the torso or total body [3]. A major challenge for combined PET/MR, aside from shielding existing PET technology from MR fields and designing new PET detectors that operate inside a magnet, is the derivation of attenuation correction factors from available MR image information [4]. In the absence of standard transmission sources employing ionizing radiation, MR-based attenuation correction (MR-AC) relies on the complete delineation of attenuating objects on the available MR images. However, standard MR sequences used for clinical acquisitions do not clearly depict tissues or objects with very short T2 relaxation times, such as MR coils or cortical bone [5].

In medical imaging, different patient positioning aids and immobilization devices are employed to assure a comfortable patient position while minimizing the risk of involuntary patient motion during the examination. It is well known from PET/CT imaging that accurate patient positioning throughout the course of the combined examination is essential for a high diagnostic quality of the images and to ensure the utmost accuracy in the spatial alignment of the PET and CT data [6, 7]. PET/MR acquisitions of the head or the torso may well take 30 min or more [8], and, therefore, proper patient support using external positioning aids is required for PET/MR imaging.

Unlike in CT imaging, the presence, extent and attenuation of these positioning aids typically cannot be described by MR. This may ultimately lead to an underestimation of the attenuation coefficients when calculated based only on the available MR images. Therefore, we studied the effects of ignoring the presence of positioning aids in PET/MR imaging scenarios.

Methods

In the absence of a whole-body PET/MR system with standard transmission sources at the time of this study, we performed all measurements on a combined PET/CT scanner. The effects of disregarding external positioning aids on MR images used for attenuation correction of complementary PET data were mimicked by segmenting and removing the positioning aids on CT images prior to CT-based attenuation correction (CT-AC) of the PET data while leaving the other attenuating objects (e.g. patient body and patient bed) unchanged.

Phantom experiments

First, a uniform 20-cm diameter cylinder filled with 40 MBq ^{68}Ge-resin was positioned centrally in the PET/CT scanner and fixed with a vacuum mattress made of a plastic bag filled with small foam pellets (additec, Germany). The air was extracted from the mattress using a vacuum pump. Thus, a maximum 10-cm thick layer was formed around the cylinder (Fig. 1a). This imaging situation mimics a head/neck study (Fig. 1c). In a second experiment, a similar cylinder phantom filled with 77 MBq ^{68}Ge-resin was placed on three foam-based MR positioning pads (Polyform, Rinteln, Germany) used in standard MR head studies. The foam structures were about 13 cm by 5 cm in size (in axial image plane) (Fig. 1b).

In both phantom experiments a single-bed PET/CT study was performed. A 256-mm scout scan was followed by a spiral CT scan (120 kVp, 5-mm slices, 16×0.75 mm, 30 mAs). The CT scan was followed by a 5-min 3-D emission scan covering the same coaxial imaging range as the CT scan.

Patient examinations

This retrospective data analysis included 16 clinical patient datasets. Of these patients, four suffered from a meningioma and were referred for a [^{68}Ga]DOTATOC-PET/CT study, five had an indication for a [^{18}F]FDG-PET/CT brain oncology examination, and seven patients were referred for a [^{18}F]FDG-PET/CT study for whole-body oncology staging or therapy monitoring. This study was approved by the local ethics committee.

All patients were examined on a PET/CT scanner (Biograph 16, HI-REZ; Siemens Healthcare, Germany). The Meningioma patients were injected with 126–151 MBq [^{68}Ga]DOTATOC and imaged 46–53 min after injection. All other patients were injected with 314–393 MBq [^{18}F]FDG and imaging started after an uptake time of 61–104 min.

For head examinations patients kept their arms by the body while the head was immobilized in a vacuum mattress (see Fig. 1c). All other patients were asked to keep their arms above the head for the duration of the combined examination while their lower extremities were fixed on a large foam pad with two half-cylinder shaped impressions

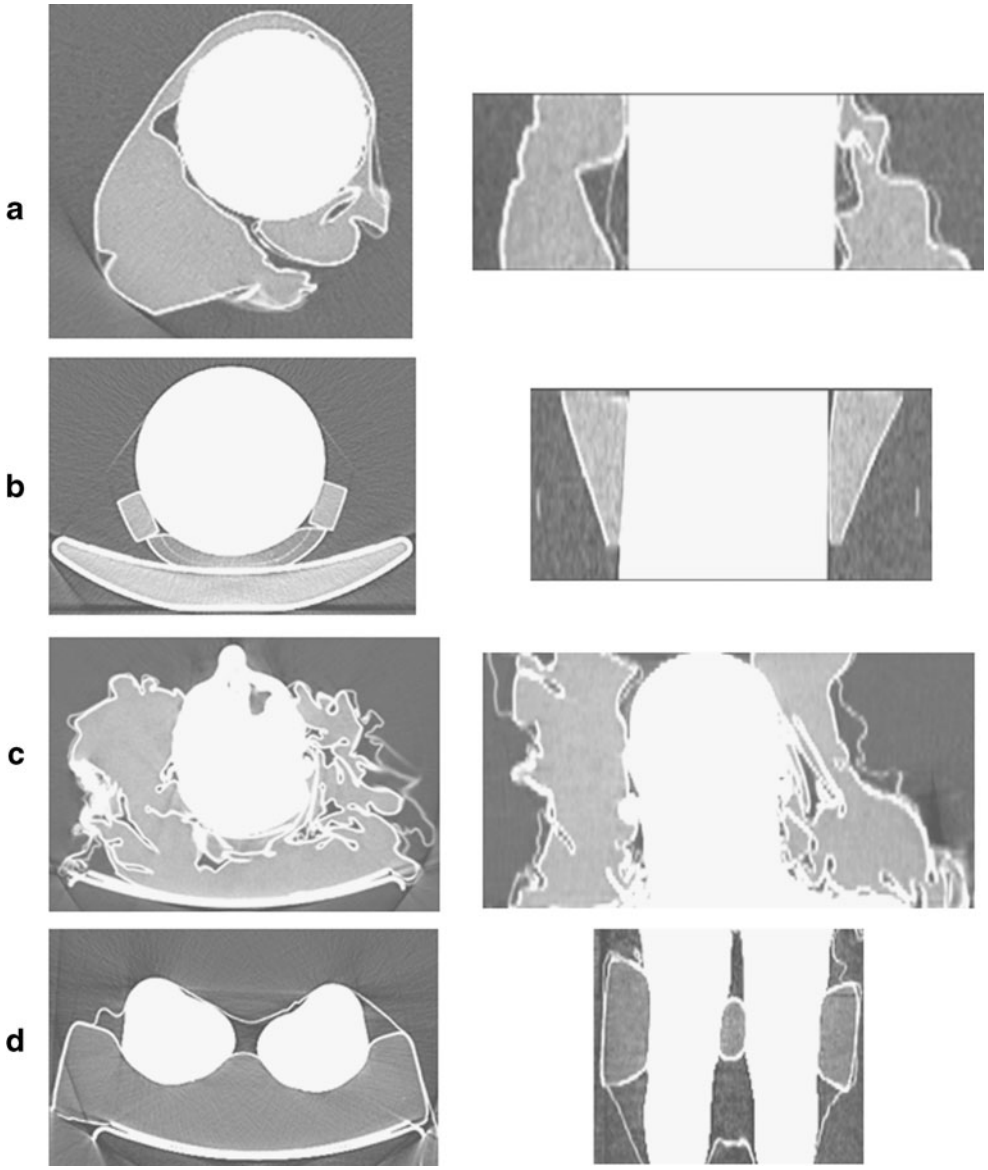

Fig. 1 Axial (*left*) and coronal (*right*) images of (**a**) the ^{68}Ge cylinder fixed in a phantom holder wrapped in a vacuum mattress, (**b**) the ^{68}Ge cylinder placed on MR positioning pads, (**c**) a head/neck patient immobilized with a vacuum mattress, and (**d**) a patient with disease of the lower extremities supported by a foam block under the knees. CT windowing was set to −950 HU (centre) and 100 HU (width)

to support the knees (Fig. 1d). A multibed PET/CT acquisition was performed, including a topogram, a spiral CT scan (120/140 kVp, 5-mm slices, 16×0.75 mm, 30–250 mAs) and a multibed (two or more bed positions for the head/neck, three or more bed positions for the lower extremities/total-body) 3-D emission scan (3 min per bed position).

Data evaluation

For each acquisition two sets of PET reconstructions were performed using different CT-AC factors. $PET_{origCT\text{-}AC}$ denotes the PET emission images following CT-AC using the originally acquired CT images without any alterations. $PET_{modCT\text{-}AC}$ denotes the PET emission images following CT-AC using the modified CT images, i.e. from which the positioning aids were removed. This corresponds to an ideal PET/MR-like imaging situation with perfect prediction of the attenuation map of the patient, but without accounting for the presence of positioning aids that typically are not seen on MR images.

The positioning aids were delineated semiautomatically based on a threshold-based segmentation of the specific foam inserts (Fig. 1b, d) or the vacuum mattress (Fig. 1a, c). The vacuum mattress was delineated automatically using a threshold algorithm in combination with morphological operations, hole filling and connected component analysis. For segmenting the foam pads beneath the knees an additional seed point was used. In all cases a modified CT attenuation map (modCT) was generated from the original CT images by setting the voxel values of the segmented positioning aids inside the measured CT field-of-view (FOV) to −1,000 HU (air), while leaving the other objects (phantom, patient body, CT patient bed, air)

unchanged. The modified CT images (modCT) were used as surrogates for MR images transformed to CT-like attenuation maps. Attenuation- and scatter-corrected PET emission data were then reconstructed iteratively (OSEM, four iterations, eight subsets, 5-mm gaussian filter) on 256×256 matrices (head/neck) and 128×128 matrices (lower extremities).

We used the PET activity concentration following measured (original) CT-AC ($PET_{origCT\text{-}AC}$) as the gold standard against which we compared PET activity concentration after modified CT-AC ($PET_{modCT\text{-}AC}$). We report voxel-based relative differences (percentages) of $PET_{modCT\text{-}AC}$ versus $PET_{origCT\text{-}AC}$ for the phantom and patient studies. In patients we restricted this analysis to voxels with a weight-based standardized uptake value (SUV) of ≥1 to reduce the influence of noise and reconstruction artefacts [9]. We also report maximum SUVs in visible lesions in the patient studies.

Results

Figure 2 shows the results of the segmentation for both phantom studies and examples of a head/neck patient and a patient with disease of the lower extremities. The average attenuation of the central vacuum mattress (Fig. 2a) was −943±31 HU, with the volume of the mattress accounting for 26% of the measured FOV. The average attenuation of the MR positioning pads (Fig. 2b) was −940 ±40 HU, while accounting for only 2.8% of the FOV.

The average attenuation of the segmented vacuum mattress across all head/neck patients was −941±4 HU, while accounting for 32% of the FOV volume on average. The average foam block attenuation for [^{18}F]FDG lower extremity examinations was −963±2 HU, while accounting for 13% of the FOV volume on average. Note, all positioning aids were enclosed in a very thin cover layer with an attenuation of between −750 HU (lower extremity support) and −830 HU (vacuum mattress).

Phantom

Figure 3 shows central axial and coronal views of the PET images of the phantom following modCT-AC and origCT-AC. When imaging the cylinder phantom on the vacuum mattress, $PET_{modCT\text{-}AC}$ image values were underestimated by 6.4% on average when compared to $PET_{origCT\text{-}AC}$; 3.4% of the $PET_{modCT\text{-}AC}$ image voxel values were underestimated by 10%, or more. In addition, a regional variation in the underestimation was observed in relation to the location and extent of the vacuum mattress, with the underestimation being more prominent in the vicinity of the vacuum mattress (Figs. 1a, 3a).

Ignoring the MR positioning aids (Fig. 1b) led to an average underestimation of 1.1% in $PET_{modCT\text{-}AC}$ following CT-AC without the positioning aids in the attenuation map;

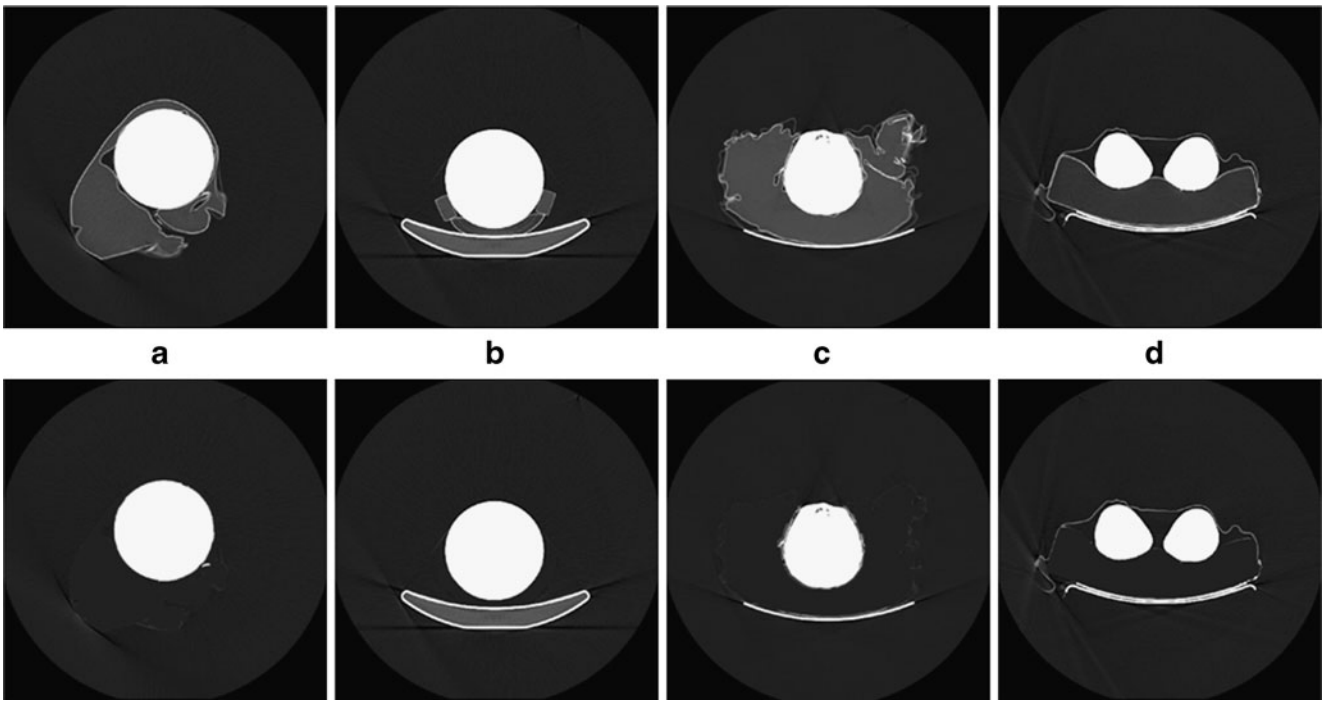

Fig. 2 Axial images of the four imaging situations: (**a**) cylinder in vacuum mattress, (**b**) cylinder on MR positioning aids (foam pads), (**c**) head/neck patient on vacuum mattress, and (**d**) lower extremities on foam block. *Top row* original CT images, *bottom row* modified CT images as surrogate MR attenuation maps. CT display in standard lung window

none of the PET voxels was underestimated by 10% or more in relation to the PET reference value (Fig. 3b). A regional variation in the underestimation, similar to the phantom positioned in the vacuum mattress, was also observed.

Patients

Figure 4 shows reconstructed axial images of a patient with head/neck cancer.

Average underestimation of $PET_{modCT\text{-}AC}$ image values versus $PET_{origCT\text{-}AC}$ across all the head/neck patients (SUV≥1) was 8.4% ([^{68}Ga]DOTATOC) and 7.4% ([^{18}F]FDG), whereby 33% and 20%, respectively of the PET voxels with SUV≥1 were underestimated by 10%, or more. As in the phantom experiments, PET underestimation was regionally variable and higher in the vicinity of the positioning aids (Fig. 4a, d).

Figure 5 shows reconstructed axial and coronal images of a patient with a lesion in the lower right leg. Average underestimation of $PET_{modCT\text{-}AC}$ image values versus $PET_{origCT\text{-}AC}$ across all seven patients (SUV≥1) was 1.9% with no PET voxel with SUV≥1 being underestimated by 10% or more. Overall deviation from reference $PET_{origCT\text{-}AC}$ was small and no significant regional variation in the underestimation was observed.

Table 1 summarizes SUVs for all visible hypermetabolic lesions in the head/neck patients. Eight of the nine patients presented with visible lesions. Lesion uptake values on $PET_{modCT\text{-}AC}$ were underestimated by 10% maximum. Table 2 summarizes activity concentrations in patients with disease of the lower extremities. Here, the underestimation from ignoring the positioning aids during attenuation correction was much smaller and less frequent than in head/neck studies.

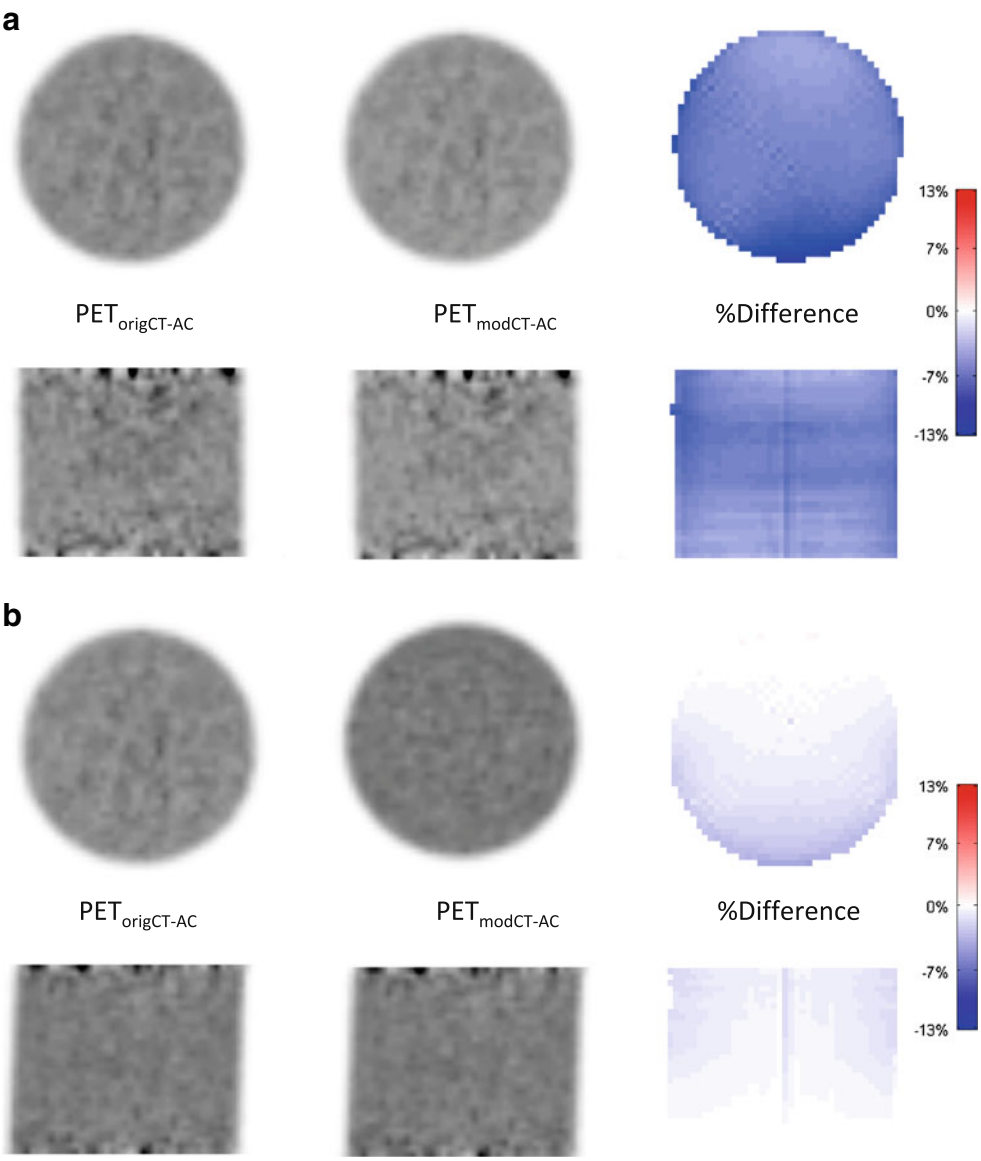

Fig. 3 Comparison of PET images of the [^{68}Ge]-cylinder with vacuum mattress (**a**) and MR positioning pads (**b**). *From left to right* PET following AC using original transmission data ($PET_{origCT\text{-}AC}$), modified transmission data ($PET_{modCT\text{-}AC}$), and PET-difference images (percentage). *Top row* axial images, *bottom row* coronal images

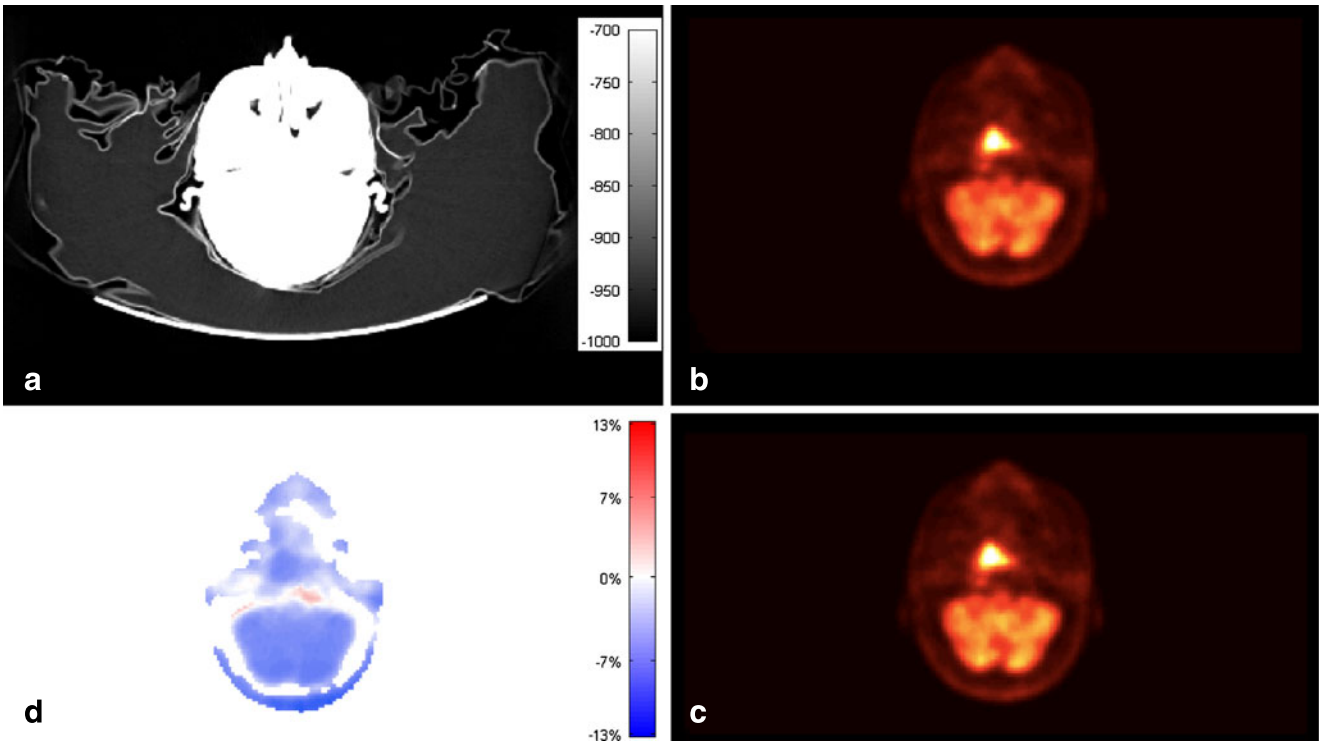

Fig. 4 [^{18}F]FDG imaging of a patient with a neck lesion, axial images: (**a**) CT with vacuum mattress (in HU), (**b**) PET following origCT-AC, (**c**) PET following modCT-AC, (**d**) difference (percent, ±13% max) image of **b** and **c**

Discussion

First experience with prototype PET/MR imaging indicates imaging times of about 30 min to 60 min, depending mainly on the coaxial imaging range and the choice of diagnostic MR imaging sequences [3, 8]. Clinical experience with dual modality PET/CT demonstrates the need for external patient support to minimize involuntary patient motion from muscle relaxation or patient discomfort during the combined examination [6, 7]. Similar positioning aids are employed in clinical MR and will be used for combined PET/MR imaging.

In contrast to CT images, and therefore PET/CT images, attenuating materials outside the patient, such as positioning aids, ancillary sensors and devices are not easily seen on MR images [10, 11]. These materials contribute to the overall attenuation of the emission signal but typically are not visible on MR images, and, thus, cannot be accounted for during MR-AC. Here, we assessed the magnitude of subsequent underestimation of the attenuation in phantom and patient studies. Our results indicate that not accounting for patient positioning aids during attenuation correction yields a noticeable bias in the PET activity concentration and introduces regionally variable distortions in the activity distribution. The overall effect depends on the actual imaging situation.

To address head and neck imaging situations, which is a likely application for combined PET/MR [12], we used phantom and patient data and explored the effects of using a vacuum mattress, a potentially suitable candidate for patient positioning in whole-body PET/MR. We observed a regionally variable underestimation of up to 22% in PET activity following AC without accounting for the attenuation of the mattress (Fig. 4). Regional variability of attenuation-corrected PET activity as a result of a poor representation of local attenuation properties has previously been described by Son et al. in brain phantom studies [13]. In our study, positioning aids provided additional but asymmetric support to phantoms and patients, and, therefore, introduced a regionally variable bias if left out of the attenuation maps. Underestimation of PET activity concentration following modCT-AC was highest in areas closest to the mattress (Figs. 2 and 4). The axial asymmetry of the MR foam pads led to a variable axial distribution of the removed attenuating material. This asymmetry correlated with the axial variation of the underestimation of the PET values following modCT-AC.

Since the PET emission data were corrected for attenuation and scatter, several voxels exhibited a small increase in activity concentration following the removal of the positioning aids from the attenuation maps (Fig. 4d). This local overestimation of central PET activity concen-

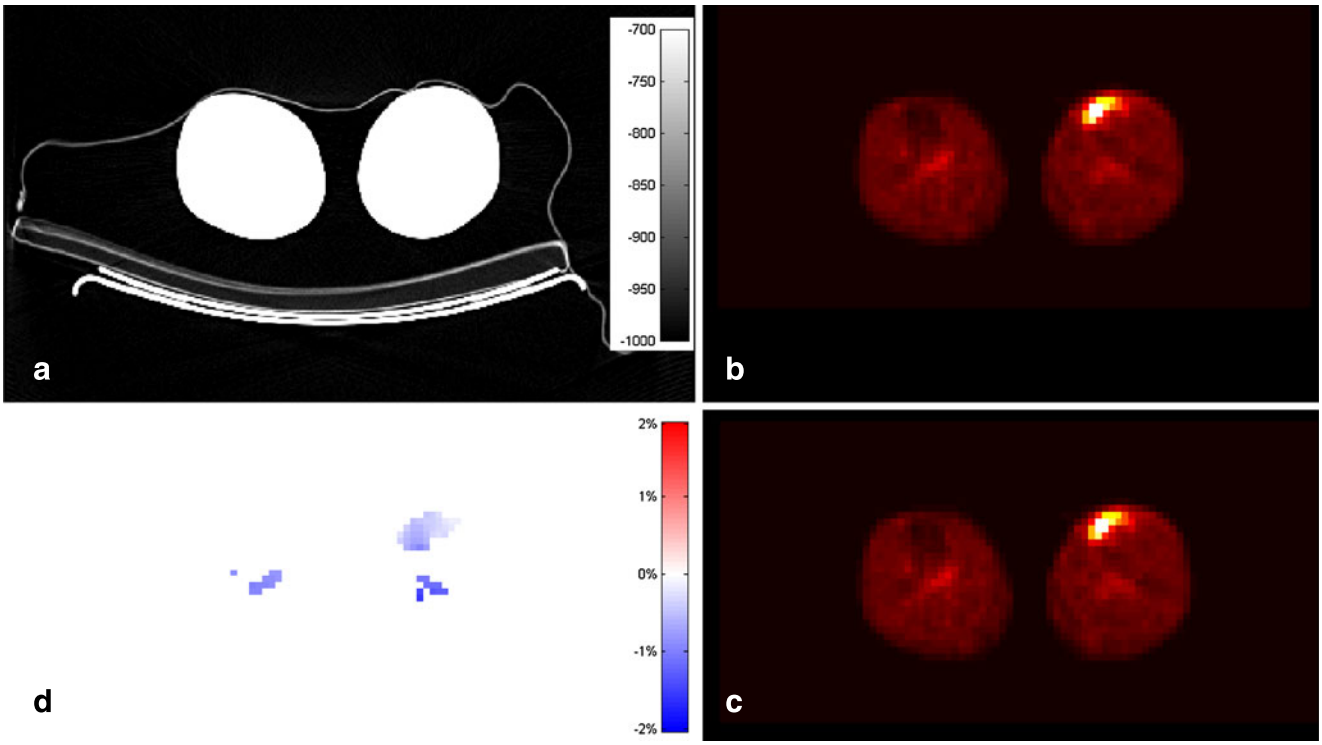

Fig. 5 [^{18}F]FDG imaging of a patient with a lesion of the lower extremities, axial images: (**a**) CT (in HU) with foam support of extremities, covered by thin blanket, (**b**) PET following origCT-AC, (**c**) PET following modCT-AC, (**d**) difference (percent, ±2% max) image of **b** and **c**

tration was not observed in PET image reconstruction without scatter correction.

When using clinically relevant patient MR positioning aids, such as the MR pads (Fig. 1b) the observed underestimation of the PET activity following AC without accounting for the MR positioning pads was small. This can be explained by the smaller contributions to the overall attenuation length as seen from a comparison of Fig. 1b and

Table 1 Maximum SUVs in lesion-based volumes of interest (VOI) for head/neck patients. VOI were defined as 50% isocontour around the hottest voxel in visible lesions. Only eight of nine head/neck patients presented with visible lesions

Patient	Tracer	$PET_{origCT-AC}$	$PET_{modCT-AC}$	Difference (%)	Lesion location
1	[^{68}Ga]DOTATOC	3.8	3.5	−8	Base of skull
2	[^{68}Ga]DOTATOC	3.1	2.8	−10	Base of skull
		3.0	2.7	−10	Base of skull
3	[^{68}Ga]DOTATOC	4.9	4.4	−11	Upper skull
		4.2	3.8	−11	Upper skull
		2.0	1.8	−10	Posterior lower brain
		3.1	2.9	−7	Anterior lower brain
		2.1	1.9	−10	Left, lower neck
		2.3	2.1	−10	Right, lower neck
4	[^{68}Ga]DOTATOC	7.4	6.7	−10	Orbit
		5.1	4.7	−8	Orbit
5	[^{18}F]FDG	5.6	5.2	−7	Left orbit
6	[^{18}F]FDG	8.6	7.9	−7	Left cervical lymph node
		12.2	11.3	−8	Right cervical lymph node
7	[^{18}F]FDG	12.6	11.4	−10	Right cervical lymph node
		4.2	3.8	−10	Neck
8	[^{18}F]FDG	12	11.2	−7	Base of skull

Table 2 Maximum SUVs in VOIs with activity concentration higher than adjacent muscle in patients with disease of the lower extremities. VOI were defined as 50% isocontour around the hottest voxel within an extended area of increased activity

Patient	Tracer	$PET_{origCT\text{-}AC}$	$PET_{modCT\text{-}AC}$	Difference (%)	Lesion location
10	[^{18}F]FDG	6.0	5.9	−2	Left knee
		1.5	1.5	0	Right knee
11	[^{18}F]FDG	1.5	1.5	0	Right knee
		1.8	1.7	−6	Left knee
12	[^{18}F]FDG	1.7	1.6	−6	Right lower knee
		1.6	1.6	0	Left lower knee
13	[^{18}F]FDG	1.4	1.4	0	Left knee
		2.2	2.1	−5	Right knee
14	[^{18}F]FDG	1.7	1.7	0	Right knee
		1.7	1.7	0	Left knee
15	[^{18}F]FDG	1.4	1.4	0	Right knee
		1.5	1.4	−7	Left knee
16	[^{18}F]FDG	1.5	1.4	−7	Right knee
		1.5	1.5	0	Left knee

Fig. 1a. However, the small positioning pads were designed to be used inside MR head coils, which serve as an additional, intrinsic positioning support. These coils contribute considerably to the overall PET attenuation [10, 14], thus rendering the contribution of the foam pads to attenuation a minor issue in clinical routine.

We also evaluated the effect of positioning aids on PET quantification of the lower extremities, which we consider another potential application of combined PET/MR in musculoskeletal imaging [15, 16]. Our data indicate a much smaller bias if positioning aids are ignored when compared to imaging of the head. Average underestimation was 1.9% with none of the pixels with SUV≥1 having a deviation of more then 10%. This can be explained partially by the lower mean attenuation of the foam pad (−963 HU vs −940 HU) and the lower overall contribution of the pads to the attenuation of all lines of response going through the lower extremities.

We also determined the maximum SUV in visible lesions in all patient studies. Similar to the average deviation in phantom studies mentioned above, we found differences of between 7% and 10% between $PET_{modCT\text{-}AC}$ and $PET_{origCT\text{-}AC}$ in head/neck patients (Table 1), while differences were mostly zero for patients with disease of the lower extremity (Table 2).

Our study was limited in that we only segmented and extracted the positioning aids within the measured transverse CT FOV (50 cm). Any attenuating components of the patient set-up and positioning aids outside the measured CT FOV were left unchanged. Therefore, our

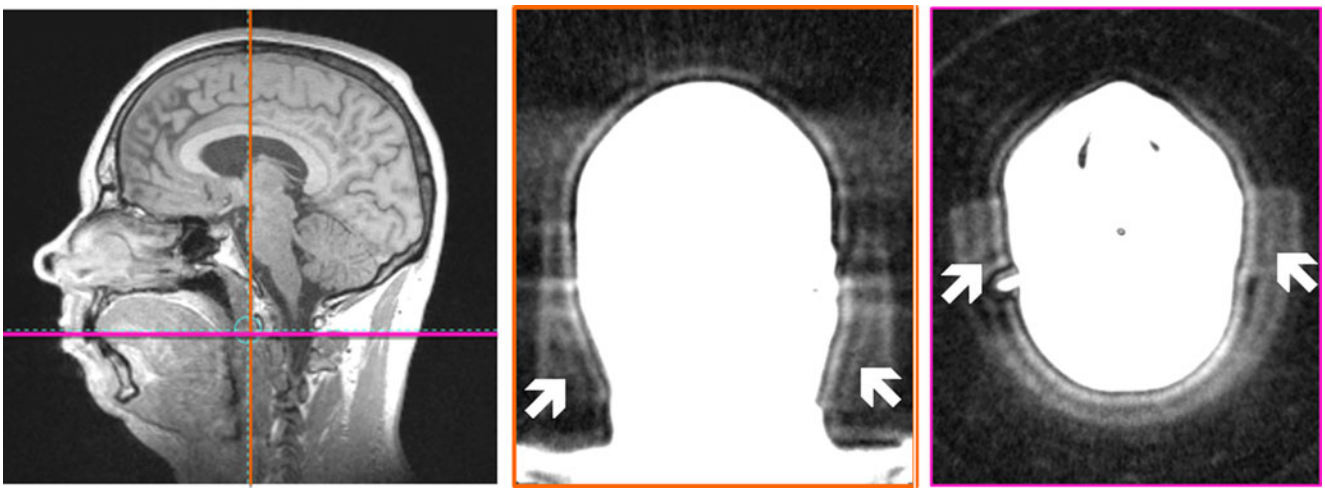

Fig. 6 Ultrashort echo time (UTE) MR imaging for visualizing extracorporeal structures such as immobilization devices. *From left to right* Sagittal scout, coronal and axial images from UTE acquisition (investigational UTE sequence with TE 0.07 ms, TR 3.56 ms, flip angle 10°, voxel size 1.25×1.25 mm, 1.25 mm slice spacing) with low threshold to enhance background visibility. The *arrows* indicate the position of the foam pads

results provide a lower estimate of the effects of the positioning aids. In addition we did not address minimal beam hardening or scatter artefacts from asymmetries in the foam-based positioning aids. Furthermore, residual local mis-segmentations remained, such as in air pockets in vacuum mattress and blankets. However, upon visual assessment their contribution to the effects studied here appeared insignificant.

Our studies showed that enough bias was introduced by larger volumes of positioning aids to affect quantification and interpretation in dedicated neurological studies; the effects were less significant when examining the extremities. It remains to be seen whether in clinical and research applications patient support for extended imaging protocols needs adapting from a standard MR positioning set-up, such as by employing vacuum mattresses (Fig. 1a, c), or whether local MR image quality needs optimization, thus leaving little room inside head and body coils for positioning devices. In any case, the bias from not accounting for foam pads and positioning aids is additive to other sources of error from predicting attenuation maps from available MR images, as discussed in [4]).

Despite the methodological challenges of MR-AC, the solution for routine PET/MR imaging is not to disregard positioning aids, but to find acquisition schemes and algorithms to delineate them on MR images acquired as part of a combined PET/MR examination. For example, dedicated MR sequences, such as ultrashort echo (UTE) sequences, are being studied for allocating and delineating bone structures [5, 14]. Whether these MR sequences could be used to delineate extracorporeal positioning aids as well would also be worth exploring. A first early attempt is shown in Fig. 6. In the future, UTE or similar sequences could be used to find the location and general extent of positioning aids [17]. For a dedicated set of positioning devices separate CT images and attenuation templates could be acquired and calculated, and matched to the estimated extent of these devices on dedicated MR images. At least for brain imaging this appears to be a viable solution for early PET/MR imaging. However, the softness and deformability of positioning aids would require a deformable alignment procedure to match the respective attenuation templates to the location in the MR images (Fig. 6).

Conclusion

A considerable and regionally variable underestimation of PET activity following attenuation correction is observed when patient positioning aids are not accounted for. This underestimation is dependent on the size and physical density of the positioning aids used. It may become relevant in combined PET/MR imaging of patients with neuropsychiatric indications, but appears to be of no clinical relevance in imaging of regions such as the lower extremities.

Acknowledgments We thank Mrs Henriette Heners for helping with the data processing and Drs. Andreas Boss, Matthias Reimold and Nina Schwenzer for helpful discussions. This study was supported in part by a grant from the German Research Foundation (DFG) PI 771/5-1.

Conflicts of Interest T.B. is founder and president of cmi-experts GmbH and reports no conflict of interest.

References

1. Pichler BJ, Kolb A, Nägele T, Schlemmer H-P. PET/MRI: Paving the way for the next generation of clinical multimodality imaging applications. J Nucl Med. 2010;51(3):333–6. doi:10.2967/jnumed.109.061853.
2. Schlemmer HP, Pichler BJ, Schmand M, Burbar Z, Michel C, Ladebeck R, et al. Simultaneous MR/PET imaging of the human brain: feasibility study. Radiology. 2008;248(3):1028–35. doi:10.1148/radiol.2483071927.
3. Ratib O, Becker M, Vallee JP, Loubeyre P, Wissmeyer M, Willi J-P, et al. Whole body PET-MRI scanner: first experience in oncology. J Nucl Med. 2010;51 Suppl 2:165.
4. Hofmann M, Pichler B, Scholkopf B, Beyer T. Towards quantitative PET/MRI: a review of MR-based attenuation correction techniques. Eur J Nucl Med Mol Imaging. 2009;36 Suppl 1:S93–104. doi:10.1007/s00259-008-1007-7.
5. Keereman V, Fierens Y, Broux T, De Deene Y, Lonneux M, Vandenberghe S. MRI-based attenuation correction for PET/MRI using ultrashort echo time sequences. J Nucl Med. 2010;51(5):812–8. doi:10.2967/jnumed.109.065425.
6. Beyer T, Tellmann L, Nickel I, Pietrzyk U. On the use of positioning aids to reduce misregistration in the head and neck in whole-body PET/CT studies. J Nucl Med. 2005;46(4):596–602.
7. Brechtel K, Heners H, Mueller M, Aschoff P, Eschmann SM, Bares R, et al. Fixation devices for whole-body 18F-FDG PET/CT: patient perspectives and technical aspects. Nucl Med Commun. 2007;28(2):141–7. doi:10.1097/MNM.0b013e328013eb09.
8. Boss A, Bisdas S, Kolb A, Hofmann M, Ernemann U, Claussen CD, et al. Hybrid PET/MRI of intracranial masses: initial experiences and comparison to PET/CT. J Nucl Med. 2010;51(8):1198–205. doi:10.2967/jnumed.110.074773.
9. Martinez-Möller A, Souvatzoglou M, Delso G, Bundschuh RA, Chefd'hotel C, Ziegler SI, et al. Tissue classification as a potential approach for attenuation correction in whole-body PET/MRI: evaluation with PET/CT data. J Nucl Med. 2009;50(4):520–6. doi:10.2967/jnumed.108.054726.
10. Delso G, Martinez-Möller A, Bundschuh RA, Ladebeck R, Candidus Y, Faul D, et al. Evaluation of the attenuation properties of MR equipment for its use in a whole-body PET/MR scanner. Phys Med Biol. 2010;55(15):4361–74. doi:10.1088/0031-9155/55/15/011.
11. Mantlik F, Hofmann M, Kupferschläger J, Werner M, Pichler B, Beyer T. The effect of positioning aids on PET quantification following MR-based attenuation correction (AC) in PET/MR imaging. J Nucl Med. 2010;51 Suppl 2:1418.
12. Antoch G, Bockisch A. Combined PET/MRI: a new dimension in whole-body oncology imaging? Eur J Nucl Med Mol Imaging. 2009;36 Suppl 1:S113–20. doi:10.1007/s00259-008-0951-6.

13. Son Y-D, Kim H-K, Kim S-T, Kim N-B, Kim Y-B, Cho Z-H. Analysis of biased PET images caused by inaccurate attenuation coefficients. J Nucl Med. 2010;51(5):753–60. doi:10.2967/jnumed.109.070326.
14. Catana C, van der Kouwe A, Benner T, Michel CJ, Hamm M, Fenchel M, et al. Toward implementing an MRI-based PET attenuation-correction method for neurologic studies on the MR-PET brain prototype. J Nucl Med. 2010;51(9):1431–8. doi:10.2967/jnumed.109.069112.
15. Nawaz A, Torigian DA, Siegelman ES, Basu S, Chryssikos T, Alavi A. Diagnostic performance of FDG-PET, MRI, and plain film radiography (PFR) for the diagnosis of osteomyelitis in the diabetic foot. Mol Imaging Biol. 2010;12(3):335–42. doi:10.1007/s11307-009-0268-2.
16. Sauter A, Horger M, Boss A, Kolb A, Mantlik F, Kanz L, et al. Simultaneous PET/MRI for the evaluation of hemato-oncological diseases with lower extremity manifestations. J Nucl Med. 2010;51 Suppl 2:1001.
17. Ladebeck R. Method for determining attenuation values of an object. US Patent Appl. No. 12/458368, Pub. No. US 2010/0007346 A1. Published Jan 14, 2010.